Optimal Demand Response Scheduling With Real-Time Thermal Ratings of Overhead Lines for Improved Network Reliability

Konstantinos Kopsidas, *Member, IEEE*, Alexandra Kapetanaki, *Student Member, IEEE*, and Victor Levi, *Senior Member, IEEE*

***Abstract*—This paper proposes a probabilistic framework for optimal demand response scheduling in the day-ahead planning of transmission networks. Optimal load reduction plans are determined from network security requirements, physical characteristics of various customer types, and by recognizing two types of reductions, voluntary and involuntary. Ranking of both load reduction categories is based on their values and expected outage durations, while sizing takes into account the inherent probabilistic components. The optimal schedule of load recovery is then found by optimizing the customers' position in the joint energy and reserve market, while considering several operational and demand response constraints. The developed methodology is incorporated in the sequential Monte Carlo simulation procedure and tested on several IEEE networks. Here, the overhead lines are modeled with the aid of either static-seasonal or real-time thermal ratings. Wind generating units are also connected to the network in order to model wind uncertainty. The results show that the proposed demand response scheduling improves both reliability and economic indices, particularly when emergency energy prices drive the load recovery.**

***Index Terms*—Optimal demand response, reliability, sequential Monte-Carlo, real time thermal rating, risk.**

NOMENCLATURE

The symbols used throughout this paper are defined below.

Indices

j	Index of generating units running from 1 to J
i	Index of load points running from 1 to N
s	Index of load types running from 1 to s_4
t	Index of hours running from 1 to T
y	Index of simulation days running from 1 to Y.

Parameters

$VOLL_i^s$	Value of lost load at load point i and load type s
$B\hat{E}DI_i$	Normalized value of expected duration interruption index in the base case
$D_i^{s\ BASE}$	Duration of interruption of load type s at load point i under the base case
$P_g^{\max}$	Maximum power output of a generation unit
$P_g^{\min}$	Minimum power output of a generation unit
$P_d^{\max}$	Maximum forecast load
$VL_i^{s,\max}$	Upper limit of the voluntary load reduction for customer type s
$IVL_i^{s,\max}$	Upper limit of the involuntary load reduction for customer type s
B	System matrix including potential contingencies
win	Per unit window for load reduction sampling
rs	Random number between {0,1}
t_{MAX}	Maximum hour limit of load recovery
f_{REC}^s	Customer's availability to recover the load
V_{ci}	Cut in wind speed
V_r	Rated wind speed
V_{co}	Cut out wind speed
P_r	Rated power output of wind turbine
$T_c(t)$	Conductor temperature at hour t
$R(t)$	AC conductor resistance at operating temperature T_c at hour t
$P_c(t)$	Convection heat loss at hour t
$P_r(t)$	Radiated heat loss at hour t
$P_s(t)$	Solar heat gain at hour t
$I(t)$	Conductor current at hour t
$V_m(t)$	Wind speed at hour t
$K_{angle}(t)$	Wind direction at hour t
$T_a(t)$	Ambient temperature at hour t.

Variables

$Pg_j(t)$	Active Power output of generation unit j at hour t
θ	Phase angles of nodal voltages
$\mu_i(t)$	Nodal marginal price of load point i at hour t
$\gamma_i^s(t)$	Slope coefficient for load recovery at node i, type s, hour t
$P_f^{\max}$	Overhead line real-time thermal rating
$P_{d\,i}(t)$	Power supplied to load point i at hour t
$\sigma_i^s(t)$	Marginal offer value for voluntary load reduction, load type s at load point i at hour t

Manuscript received April 26, 2015; revised August 22, 2015 and November 27, 2015; accepted March 6, 2016. Date of publication April 1, 2016; date of current version October 19, 2017. This work was supported by the Engineering and Physical Sciences Research Council within the HubNet Project under Grant EP/I013636/1. Paper no. TSG-00463-2015.

The authors are with the School of Electrical and Electronic Engineering, Electrical Energy and Power Systems Group, University of Manchester, Manchester M13 9PL, U.K. (email: k.kopsidas@manchester.ac.uk; alexandra.kapetanaki@manchester.ac.uk; victor.levi@manchester.ac.uk).

Color versions of one or more of the figures in this paper are available online at http://ieeexplore.ieee.org.

Digital Object Identifier 10.1109/TSG.2016.2542922

$VL_i^s(t)$	Amount of voluntary load reduction of load type s at load point i at hour t
$IVL_i^s(t)$	Amount of involuntary load reduction of load type s at load point i at hour t
$D_i^s(t)$	Duration of interruption of load type s at load point i at hour t
$Pc_i^s(t)$	Total load shedding of load type s at load point i at hour t
$f_{RED}^s(t)$	Load type s availability to respond to a demand response call at hour t
$CVL_i^s(t)$	Contracted voluntary load reduction of load type s at load point i at hour t.

Functions

$GR_j(\cdot)$	Revenue of generator j
$LC_i(\cdot)$	Cost of delivered demand at node i
$VLR_i(\cdot)$	Revenue for voluntary load type s reduction at node i
$IVLR_i(\cdot)$	Revenue for involuntary load type s reduction at node i
$\hat{R}_i^s(\cdot)$	Ranking order for load type s at node i
$[\Lambda^-]_i^s(\cdot)$	Size of load reduction for load point i type s
$[\Lambda^+]_i^s(\cdot)$	Size of load recovery for load point i type s
$Savings_i^s(\cdot)$	Customer savings for load point i type s in the event that demand response materializes
$C^s_{payback\ i}(\cdot)$	Payback cost due to load recovery at node i type s
$\pi_i^s(\cdot)$	Profit of load customer at load point i type s
$VaR_a^{NR}(\cdot)$	Value at risk for network rewards at confidence level α
$VaR_{1-\alpha}^{NC}$	Value at risk for network costs at confidence level *1-*α
$P(\cdot)$	Wind turbine power output for wind speed V_m.

I. Introduction

THE EVER increasing integration of intermittent renewable energy into the electricity network, combined with a constantly growing demand, is likely to cause much greater stress on existing networks increasing the probability of severe contingencies [1]. To avoid this, several preventive and corrective actions, including demand response (DR), spinning reserve scheduling, application of real-time thermal ratings (RTTR) and energy storage scheduling, can be deployed to relieve stress in particular areas of the network.

DR strategies currently under investigation consider distribution level [2], [3], but their potential in transmission networks is often overlooked. Research related to the impact of DR on network reliability is very limited [4]–[6]. The model proposed in [5] evaluates short term operational benefits in terms of generation and interrupted energy costs from interruptible loads by using the contingency enumeration technique; however, it does not fully address the customer perspective because there is no modelling of load recovery and associated costs, characteristics of different load and DR types and probabilistic nature of available interruptible demand. Even if a probabilistic approach is used to assess the DR contribution [6], only single contingencies are analysed.

Physical characteristics of different types of load customers need to be adequately represented in the studies. Domestic and small commercial loads are analysed in [7]–[9] but fail to assess how critical each customer type is for a network's load point in terms of interruptions. Next, examining different sizes and shapes of both load reduction and recovery is essential for a complete and accurate network assessment; however, load recovery is usually ignored in the studies [4]. Load reduction and recovery can be based on electricity market prices in order to eliminate price spikes during peak hours [4], [10]. However, these studies often ignore operational and security constraints of the transmission networks and are run for intact networks only. Enumeration techniques, as opposed to Monte Carlo simulation, are often used to calculate the DR contribution, and thus fail to include the whole set of contingencies and a number of uncertainties a network might experience [11]. Finally, instead of applying DR every time a contingency occurs, DR should only be used when the reliability is improved and when savings are higher than the expected payback costs.

This paper proposes a probabilistic approach for optimal demand response scheduling in the day-ahead planning of transmission networks. Uncertainties related to forecast load, network component availability, available amount of demand response and wind speeds are incorporated into the sequential Monte Carlo simulation framework. Synchronous and wind generating units, as well as four types of load customers (large, industrial, commercial and residential) are modelled. Optimal nodal load reductions are calculated using the optimum power flow model, and are then disaggregated into voluntary and involuntary components. Recognizing that directly-controlled loads can certainly be shed and indirectly-controlled contain a probabilistic component, optimal amounts of voluntary and involuntary nodal reductions are determined. Different load recovery profiles for customer types are considered next within 'payback periods' and they are initiated when the load customer's revenue is highest. Here, delivered load is priced at nodal marginal price, voluntary load reduction at marginal offer price and involuntary load reduction at damage cost. The whole analysis is implemented from the load customer's perspective to maximise their revenues, whilst the load recoveries are controlled by the transmission system operator (TSO); they may represent either physical paybacks from specific appliances or controlled paybacks whereby the TSO schedules its customer loads so as to have the desired shape. The benefits of optimal DR strategies are evaluated in combination with real-time thermal ratings of overhead lines to reveal the true potential of the DR. The outputs of the model also include financial risk quantifiers that the revenues are below, or costs are above a threshold.

II. Overview of the Methodology

Optimal DR scheduling is determined using the sequential Monte Carlo probabilistic approach. The main features of the proposed DR modeling framework are: a) Load reduction scheduling driven by network security; b) Optimal scheduling of load recovery using economic criteria; c) Modelling of real-time thermal ratings of overhead lines;

and d) Modelling of renewable energy sources, such as wind generation.

The overall methodology is realized within two independent sequential Monte Carlo simulation (SMCS) procedures. The first SMCS is the initialization module, which is used to calculate several components required by the second SMCS that determines optimal day-ahead operation of the power system. The main building blocks of the first SMCS procedure are: a) Calculation of reliability indices needed for ranking of load types for demand reduction; b) Calculation of real-time thermal ratings of overhead lines; and c) Determination of nodal marginal prices and several economic indicators used for finding the optimal schedule of load recoveries.

The second SMCS consists of four modules: a) Demand reduction scale module; b) Load recovery scale module; c) Demand reduction and load recovery (DRLR) control module, and d) The outputs module. The first module contains ranking of different load types for demand reduction, calculation of required amounts of voluntary and involuntary DR, as well as the customer revenues. The load recovery scale module considers load recovery profiles and sizes, and determines a matrix with the most appropriate schedule hours for load recovery. The DRLR-control module contains logics for initiation of load reductions and load recoveries, whilst the outputs module includes optimal load reduction and recovery schedules, as well as reliability and financial indicators.

III. Methodology

The proposed demand scheduling methodology is aimed at determining the optimal demand response plan for the next day, when the committed generation units, status of network switching devices and forecast loads are well defined. However, several uncertainties in the day-ahead operation are still present, so that the overall problem is formulated as a probabilistic model and solved with the SMCS. The proposed DR methodology is applied for post contingency states; however it is general enough to also consider pre-contingency events. The main building blocks are briefly presented below.

A. Sequential Monte Carlo Simulation

Sequential Monte Carlo simulation performs analysis of time intervals in chronological order whilst taking into account various uncertainties [11]. It can model the chronological phenomena, such as load reduction and recovery, real-time thermal ratings and wind generations. Following uncertainties were assumed for a day-ahead operation of the transmission network:

- Load varies in a window around the forecast hourly loads. The uncertainty window is defined by the MAPE of the short-term forecast by hourly intervals obtained using the neural network approach [12].
- Availability of all generation and network units was modelled with the aid of two-state Markovian model with exponentially distributed up and down times [11].
- Wind speed hourly predictions and a window around the predicted values are applied within the random sampling. An alternative approach is to use wind speed probability distribution functions (PDFs) by hourly periods.
- Amount of voluntary load reduction that varies by customer and DR type. For example, DR from residential customers responding to price signals is highly uncertain, whilst DR from incentive-based contracted commercial customers has much less uncertainty – see Section III-D.

One SMCS period is equal to 24 hours and simulations are repeated until convergence is obtained. Any failure that goes over the planning horizon (i.e., 24:00) was considered in the 'next day' simulation. The same simulation principles were applied in both SMCS procedures.

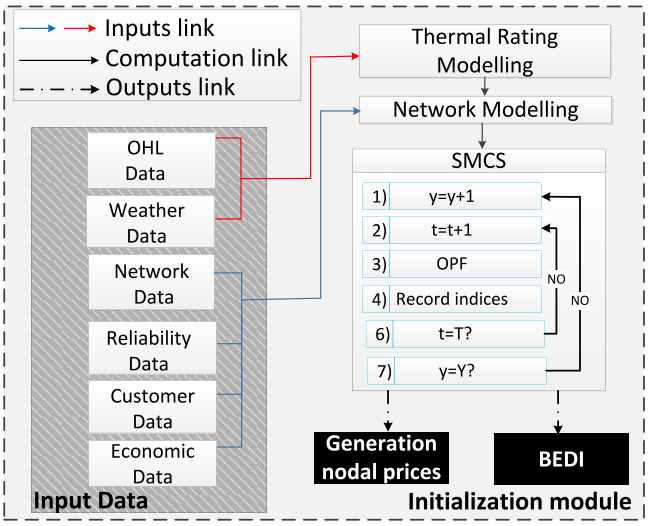

Fig. 1. Computations within the initialization module.

B. Initialization Module

The initialization module is used to calculate several quantities required by the main simulation loop. Following the data input, network model with real-time thermal ratings and load customer characteristics is built and fed into the first SMCS procedure, as shown in Fig. 1. The outputs from this stage are some pricing and reliability indicators.

1) Input Data: The input data include network, reliability, customer, economic data, overhead line (OHL) data and weather data. Beside the standard network data, forecast in-service generation units with technical characteristics and chronological hourly load point demands are input. Reliability data are failure rates and repair times of all components, whilst customer data encompass customer and DR types, contracted voluntary load reductions, normalized load recovery profiles and customer availability to respond to a DR call. Essential economic data are generation costs, values of lost load (VOLL) and marginal offer prices for voluntary load reduction. Average VOLL data by customer types were obtained from the latest U.K. national study [13].

Weather data include ambient temperatures, wind speeds and directions required for the calculation of RTTRs of OHLs, as well as either forecast hourly wind speeds or hourly wind speed PDFs used to calculate wind generations. Several other

OHL construction and heat dissipation/gain data are further required to calculate RTTRs.

The input data are fed into the thermal ratings and network modelling modules, whose outputs are then used by the SMCS procedures.

2) Thermal Ratings of Overhead Lines: Two different OHL rating models are used in the developed simulation procedures, the 'seasonal' thermal rating (STR) and the RTTR. The STR is defined by seasons and for different design conductor temperatures [14]. The lowest ratings are for summer conditions and design temperature of 50°C [15]; they are of conservative nature.

To get the RTTRs, it is possible to do a thermal analysis on an hourly basis. Assuming a steady-state thermal equilibrium is achieved in each hourly period, static thermal balance is achieved by equating heat dissipated by convection and radiation (or 'cooling') with solar and Joule heat generated. In the applied IEEE model [15], the convection heat loss varies with the change in wind speed (V_m), wind direction factor (K_{angle}) and the difference between the conductor (T_c) and ambient air temperature (T_a). The radiation heat loss is the energy of the electromagnetic waves emitted to the ambient space; it is a function of the temperature difference between the conductor and air, and the emissivity of the conductor. The solar radiation is a function of several parameters including solar azimuth, total radiated heat flux rate, etc. Finally, Joule (I^2R) losses are calculated in the standard way using AC resistance dependent on conductor temperature, so that the RTTR of OHLs is determined as:

$$I = \sqrt{\left(P_c\left(T_c, T_a, K_{angle}, V_m\right) + P_r(T_a, T_c) - P_s\right)\big/R(T_c)} \quad (1)$$

where $P_c(\cdot)$ is the convection heat loss, $P_r(\cdot)$ is the radiated heat loss, P_s is solar heat gain and $R(T_c)$ is the conductor resistance at operating temperature T_c. The conductor temperature needs to be set to one of the standard design values (i.e., 50°C, or 65°C, or 75°C) to get the OHL ampacity; an increased value can be used during system emergencies.

The average values of 5-year hourly weather data were obtained from the BADC MIDAS metheorogical stations for Aonach, U.K. [16]. The rest of the required data were obtained from the U.K. consultants.

3) Analysis Within the SMCS Procedure: The initialization module is used for two purposes; the first is to determine the base expected duration interruption (*BEDI*) index of loads needed for ranking of loads within the demand reduction scale module. The second is to compute the probabilistic energy nodal prices used within the DRLR-control module to find the optimal load recovery strategy. The probabilistic nodal prices at different confidence intervals α are further analysed to make decision about the most appropriate load recovery times.

Each hour within the simulation period is characterized by available generating units, transformers and circuits, as well as nodal loads and operational constraints. An optimum power flow (OPF) model is solved to find the levels of voluntary and involuntary load reductions and revenues to generator and demand customers. The formulation of the OPF model is a modification of the market-clearing model proposed in [17]; the main difference is that there is no preventive control and corrective scheduling is applied to the already sampled contingent case. Mathematical formulation of the model is:

$$\text{Min} \quad \left\{ \sum_{\text{j}\in\text{J}} \text{C}_{\text{g j}} \cdot P_{gj} + \sum_{i\in I}\sum_{s\in S} VOLL_i^s \cdot IVL_i^s + \sum_{i\in I}\sum_{s\in S} \sigma_i^s \cdot VL_i^s \right\} \quad (2)$$

$$\text{subject to:} \quad P_g - P_d - B\theta = 0 \quad (\mu) \quad (3)$$

$$P_f = H\theta \quad (4)$$

$$-P_f^{\max} \le P_f \le P_f^{\max} \quad (5)$$

$$-P_g^{\min} \le P_g \le P_g^{\max} \quad (6)$$

$$0 \le VL_i^s \le VL_i^{s,\max} \quad (7)$$

$$0 \le IVL_i^s \le IVL_i^{s,\max} - VL_i^{s,\max} \quad (8)$$

$$P_d^{\max} - \sum_s IVL^s - \sum_s VL^s \le P_d \le P_d^{\max} \quad (9)$$

The objective function to be minimized (2) is the sum of the offered cost functions for generating power plus the sum of the cost of involuntary load reduction for all load nodes and types plus the sum of offered costs for voluntary load reduction for all load nodes and types. The involuntary load reduction is valued at *VOLL* that is dependent on the general load type; dependency on the connection node is taken into account because there may exist special loads whose curtailment must be avoided. Voluntary load reduction is priced at the rates offered by consumers to provide this service. They are closely linked to the offers made by generators for the 'up-spinning reserve' in the joint energy and reserve market [17]. It is again envisaged that the rates can vary with customer type and connection location. Finally, note that time index t is avoided for simplicity.

Using a dc load flow model, constraints (3) represent the nodal power balance equations for the considered state, which includes potential contingencies within the system matrix B. A Lagrange multiplier (or dual variable) μ_i is associated with each of the equations. Constraints (4) express the branch flows in terms of the nodal phase angles, while constraints (5) enforce the corresponding branch flow capacity limits. Here, modelling of OHL ratings can be done using the RTTR model, in which case limit ${P_f}^{max}$ is a function of the time step t.

Constraints (6) set the generation limits for the considered state, while considering available units and requirements for the down- and up-spinning reserve in the analysed time step [17]. Reserve requirements depend on the system load and contingency state [17]. For the non-controllable units, such as wind turbines, upper and lower limits are the same.

Constraints (7), (8) and (9) set the limits of the demand; they are expressed as inequality constraints on the voluntary and involuntary load reductions and the total delivered load. The upper limit of the voluntary load reduction $VL_i^{s,\max}$ can contain a probabilistic component for some DR types and is dependent on the considered time step. As a consequence, the upper limit of the involuntary load reduction is the difference between of the absolute limit $IVL_i^{s,\max}$ and the voluntary load reduction

limit $VL_i^{s,\max}$. Finally, the delivered demand P_d is equal to the forecast load in the considered time interval P_d^{max} if there is no load reduction. The lower limit is specified in terms of the forecast load, voluntary and involuntary load reductions, which are a part of the optimal solution.

Solving the optimization model (2) to (9) gives the optimal values of the unknown variables, as well as dual variables associated with the constraints of this problem [18]. The significance of the dual variables is discussed below.

4) Nodal Marginal Costs: The optimal solution of the problem (2) to (9) is equal to the optimal solution of the corresponding dual problem whose unknowns are dual variables associated with the constraints (3) to (9) [18]. The objective function of the dual problem is a sum of products of the dual variables and the right-hand sides of the constraints, showing that the total optimal cost can be recovered in another way using the dual variables as charging rates. The dual variables represent the additional cost of changing the right-hand side of the constraints by unity; they are therefore called marginal costs or prices [19].

Dual variables μ are the nodal marginal costs of meeting the power balance at each system node for the considered operating regime. The nodal marginal costs have been extensively used for electricity energy and reserve pricing [6], [9], [20]. The nodal marginal prices vary over the system nodes and during the day due to load variation and congestion in the system [21]. The greatest variation of marginal prices is experienced due to unexpected failures of lines and/or generator units [6]. Consequently, these prices should be carefully considered for the load recovery scheduling.

In our approach, we have applied a concept similar to the real time pricing scheme proposed in [22]. The following quantities are calculated in each time step t:

- The revenue of generator j:

$$GR_j(t) = Pg_j(t) \cdot \mu_j(t) \tag{10}$$

- The cost of demand i delivery:

$$LC_i(t) = P_{d\,i}(t) \cdot \mu_i(t) \tag{11}$$

- Revenue for voluntary load i reduction:

$$VLR_i(t) = \sum_{s=1}^{s4} \left(\sigma_i^s(t) \cdot VL_i^s(t)\right) \tag{12}$$

- Revenue for involuntary load i reduction:

$$IVLR_i(t) = \sum_{s=1}^{s4} \left(VOLL_i^s \cdot IVL_i^s(t)\right) \tag{13}$$

We have defined *VOLL* by load types in the initialization module, as presented in equation (13). However, in the second SMCS there is an option to use a look-up table where *VOLLs* are functions of interruption duration [23]. The interruption duration is estimated as:

$$D_i^s = \begin{cases} mean\left(D_i^{s\ BASE}\right), & if\ D_i^s \le mean\left(D_i^{s\ BASE}\right) \\ D_i^s, & if\ D_i^s > mean\left(D_i^{s\ BASE}\right) \end{cases} \tag{14}$$

where $D_i^{s\ BASE}$ denotes the interruption duration calculated in the initialization module. The estimated duration of interruption is equal to the mean base value unless the interruption already lasts for more than the base value; it then takes the actual duration value.

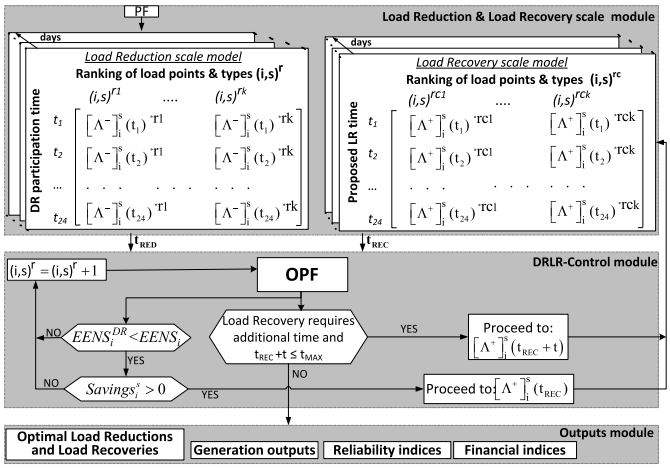

Fig. 2. Optimal demand response computational framework.

C. Optimal Demand Response Scheduling

The computational framework for optimal demand response scheduling is illustrated in Fig. 2. The load reduction and recovery scale modules feed into the DRLR control module. Ranking of different load types and calculation of *available* sizes for voluntary load reduction is performed within the load reduction scale module. The order of ranking the load points and types is represented by $(i, s)^r$ in Fig. 2. Hence, in the load reduction matrix, if load reduction takes places at hour t_1 the load reduction of $(i, s)^{r1}$ customer will be evaluated first, while the $(i, s)^{rk}$ customer will be evaluated at the end.

The load recovery scale module computes the most appropriate schedule hours for load recovery, as well as the potential recovery sizes and profiles. The order of ranking the load points and types is represented by $(i, s)^{rc}$ in Fig. 2. Hence, in the load recovery matrix, if load recovery takes places at hour t_1 the load reduction of $(i, s)^{rc1}$ customer will be evaluated first, while the $(i, s)^{rck}$ customer will be evaluated at the end. Both load reduction and recovery are managed by the DRLR control module in which the OPF is used to determine optimal voluntary and involuntary load reductions, and the developed control scheme gives the optimal load recovery profiles. The outputs module finally gives optimal DR and LR schedules, as well as financial and reliability indicators.

D. Load Reduction Scale Module

Load reduction scale module is required for each load point and load type when load shedding takes place at the considered hour t_{RED}. The physics of demand response are presented first, which is followed by the ranking and sizing.

Four load types, industrial, commercial, large user and residential, have been defined in our approach. Different characteristics have been associated with these four types, such as temporal load variations, total amounts available for

voluntary and involuntary load reductions, relative load recovery profiles and economic data. Two categories of demand response have been recognised, namely direct and indirect load control [24]. In direct load control, the contracted customers (usually large and industrial) are directly disconnected during emergency conditions and they receive revenue for participating in the 'reserve market' [25]. The contracted amounts are certain and they are of deterministic nature. In indirect load control, incentive- and price-based demand responses can be distinguished. The former group refers to the customers contractually incentivised to curtail load during system emergencies [26], [27]. This category can be considered semi-probabilistic; we have used sampling within a window around the contracted value. Finally, in price based demand response customers move their consumption from periods of higher to periods of lower prices. This demand response is a probabilistic quantity which can vary from zero up to the estimated maximum amount.

Load ranking at each node i and for each load type s at the considered hour t_{RED} is based on the financial implications of reducing the load. The ranking order is a product of the normalized value of the base expected duration interruption index ($BEDI_i$) calculated in the initialization module, the normalized marginal offer price $\hat{\sigma}_i^s$ for voluntary load reduction or customer interruption cost $VOLL_i^s$ for involuntary load reduction, and the required load shedding Pc_i^s. This is shown in relations below:

$$\hat{R}_i^s(t_{RED}) = \begin{cases} \hat{BEDI}_i \cdot Pc_i^s \cdot \hat{\sigma}_i^s, & \textit{voluntary load} \\ \hat{BEDI}_i \cdot Pc_i^s \cdot VOLL_i^s, & \textit{involuntary load} \end{cases} \quad (15)$$

$$BEDI_i = \sum_{y=1}^{Y} \sum_{t=1}^{T} \sum_{s=1}^{s_4} \zeta_i^s \cdot D_i^{s\ BASE} \Big/ Y \quad (16)$$

Relation (15) shows that independent ranking lists for voluntary and involuntary load reductions can be built. Ranking of all 'voluntary customers' is based on submitted marginal offer prices, which can be normalised with the average price of up-spinning reserve in the energy-reserve markets [17]. On the other hand, involuntary load reductions are ranked using *VOLL*. The *VOLL* is defined either by load types, or customer damage functions are used; it is normalised using the average VOLL in the entire GB [13]. The base expected interruption index $BEDI_i$ is found from the number of interruptions ζ_i^s having duration $D_i^{s\ BASE}$ across the entire simulation period.

The total required amount of load reduction Pc_i^s is determined from the OPF model and it consists of voluntary and involuntary components. When considering industrial and large customers under the direct load control, it was assumed that available voluntary load reduction is equal to the contracted voluntary reduction (CVL_i^s). Then the (part of) voluntary load reduction is:

$$\left[\Lambda^-\right]_i^s(t_{RED}) = \begin{cases} Pc_i^s(t), & \textit{if } Pc_i^s(t) < CVL_i^s(t) \\ CVL_i^s(t), & \textit{if } Pc_i^s(t) > CVL_i^s(t) \end{cases} \quad (17)$$

Available voluntary load reductions from industrial and commercial incentivised customers and residential customers contain a probabilistic component that can be determined using random sampling. It is calculated using the availability factor f_{RED}^s:

$$f_{RED}^s = \begin{cases} 1 + (rs - 1)win, & \textit{industrial \& commercial} \\ rs, & \textit{domestic customers} \end{cases} \quad (18)$$

where rs is a random number generated from the uniform distribution between {0,1} and win is the per unit window. In case of incentivised (industrial and commercial) customers, the available amount is based on average probability that the contracted amount is available; for example, if the probability is 0.9 then $win=0.2$. Residential customers respond to price signals and the uncertainty window is the entire available range. The available voluntary load reduction is then calculated by multiplying the availability factor (18) and the contracted value (CVL_i^s) in case of incentivised industrial and commercial customers, or estimated maximum load reduction of residential customers.

After having obtained *available* voluntary load reductions for all types of customers s at node i, the total voluntary and involuntary load reductions are calculated using the ranking order and a relation similar to expression (17). The minimum amount of involuntary load reduction is always used to meet the network security constraints.

E. Load Recovery Scale Module

This module determines the amounts of *potential* load recoveries in the period following load reduction in time slot t_{RED}. The actual load recovery is determined in the DRLR control module using the hourly nodal marginal prices.

Load recovery profiles can be very different for the considered customer types, and moreover, for different customers within a single group; a good example is industry [28]. We applied a general normalized load recovery profile of triangular shape, which is modelled by two straight lines in discrete form. The upward line models load pick-up after the customer reconnection, whilst the downward line brings it back from the 'overshot point' to the pre-disconnection value. The discrete modelling is done using the upward/downward slope coefficients in consecutive time intervals.

The amount of load recovery at time period $t_{REC} + t$, $[\Lambda^+]_i^s(t_{REC} + t)$, is computed by using the following expression:

$$\left[\Lambda^+\right]_i^s(t_{REC} + t) = \left[\Lambda^-\right]_i^s(t_{RED}) \cdot \gamma_i^s(t_{REC} + t) \cdot f_{REC}^s \quad (19)$$

where $[\Lambda^-]_i^s(t_{RED})$ is amount of load reduction of load type s at node i, $\gamma_i^s(t_{REC} + t)$ is upward or downward slope coefficient and f_{REC}^s is the availability factor of type s load recovery. This factor was introduced because not all customers may come back when supplies are restored or signalled [29]. In the current approach, availability factors f_{REC} are deterministic quantities defined by customer types and network nodes. It is also worth noting that the load recovery can be higher than the amount of the initial load reduction [28]; the slope factors can take values greater than unity.

Modelling of load recovery profiles over a specified time period introduces additional complexities in the developed SMCS methodology. Each time a load recovery is initiated, the corresponding nodal load needs to be modified over a specified

period in line with the load recovery profile. Besides, a record must be kept of all load recoveries at different time steps, because they cannot be considered for further load reduction. This is reflected in the next DRLR module.

F. Demand Reduction Load Recovery Control Module

The DRLR control module is used to control the initiation of load reductions and recoveries and to produce their optimal schedules within the forecast 24 hourly period. Some of the control principles are listed below:

- Loads whose recovery process is underway cannot be considered for load reduction.
- Loads eligible for load reduction will not be disconnected if there is no improvement in the energy-not-served following the load reduction.
- Only those loads, whose reduction including recovery generates revenue to the customers, will be actually disconnected and reconnected.
- The best timing of load recovery is determined using the (forecast) nodal marginal prices over the recovery period.

Assume the OPF analysis has generated non-zero load curtailments. Those loads which are not a part of previous load recoveries are ranked and sizes of voluntary and involuntary reductions are determined. The first load reduction from the ranking list is applied and it is checked with the aid of the OPF whether the total energy-not-served has reduced. If this is the case, the nodal customer *profits* are computed based on the *savings* acquired due to the load reduction and the projected *payback cost* due to the load recovery. The optimum load recovery always takes place when the nodal marginal prices are 'low' over the recovery window. If the load customer projected profit is negative, the load reduction is not activated even if the reliability of the network might improve.

Calculation of customer savings, costs and profits is briefly presented below.

1) Customer Savings: The customer savings incurred during load reduction are the consequence of reduced load payments to the generators. These payments are valued at nodal marginal prices $\mu_i(t)$, as shown in equation (11), which are in turn dependent on the considered regime. The customer savings are therefore calculated from two OPF runs: the first without load reduction and the second with load reduction. The change in load payments, ΔLC, represents the customer savings at t_{RED}:

$$\Delta LC_i^s(t_{RED}) = LC_i^{s\ NO-DR}(t_{RED}) - LC_i^{s\ DR}(t_{RED}) \quad (20)$$

The total savings are then found for the entire interval when the load reduction is in place:

$$Savings_i^s(t_{RED}) = \sum_{t=t_{RED}}^{t_{REC}} \Delta LC_i^s(t) \quad (21)$$

2) Payback Costs: If customer *savings* are positive then the algorithm proceeds to the load recovery stage to project the optimal load recovery schedule. The optimization is based on the following principles:

- Load recovery is always scheduled after the corresponding load reduction and it can continue into the 'following' simulated day. There are periods within a day when the load recovery does not take place; for example between 12am and 5pm on weekdays for residential customers.
- Load recovery blocks due to involuntary load reduction are always committed before voluntary load recovery blocks. They are prioritized based on their VOLL; where the VOLL is the same, ranking is based on the size of load reduction, the largest loads being reconnected first. Similar criteria are applied to voluntary load reductions, where marginal offer prices are used instead of VOLL.
- Optimal timing of load recovery is determined by finding the weighted average of (base) nodal marginal prices over the recovery window. The weights are equal to the slope coefficients $\gamma_i^s(t_{REC}+t)$ of the normalized recovery profile. The window with the smallest average nodal marginal price is selected for the load recovery. This approach is the best for load customers, because they will be exposed to the least additional payback cost.
- After having determined the optimal starting hour of load recovery, it will only be materialized if there will be no new load curtailments within the recovery window. This is checked by running OPF over consecutive time periods within the recovery window; where curtailments occur, the next best recovery window is examined and so on.

The payback costs due to the selected optimal load recovery schedule are again computed from two OPF runs in each time step within the recovery window. Since load recovery increases the amount of load, additional cost ΔLC is calculated as the difference between costs with and without load recovery over the load recovery period t_{REC} to t_{MAX}:

$$\Delta LC_i^s(t_{REC}) = LC_i^{s\ DR}(t_{REC}) - LC_i^{s\ NO-DR}(t_{REC}) \quad (22)$$

$$C_{payback\ i}^{s} = \sum_{t=t_{REC}}^{t_{MAX}} \Delta LC_i^s(t) \quad (23)$$

3) Customer Profits: The total customer profit $\pi_i^s(t_{RED})$ needs to account for savings due to reduced load, costs due to load recovery, as well as rewards for voluntary and involuntary load shedding. This is summarised in the equation below:

$$\pi_i^s(t_{RED}) = Savings_i^s - C_{payback\ i}^{s} + \sum_{t=t_{RED}}^{t_{REC}} IVLR_i^s(t) + \sum_{t=t_{RED}}^{t_{REC}} VLR_i^s(t) \quad (24)$$

Only load customer with a positive profit $\pi_i^s(t_{RED})$ evaluated at time t_{REC} proceeds into the DR strategy. The analysis continues until the convergence criterion on expected energy not served is met. After having completed the SMCS procedure, the algorithm goes straight to the outputs module.

G. Outputs Module

The outputs module generates several results related to the load reductions, nodal prices, generation outputs, reliability and financial indicators. They are briefly discussed below.

1) Optimal Load Reductions and Recoveries: PDFs of voluntary and involuntary load reductions by load types and/or nodes are calculated for each hour in the 24-hourly period. These can be directly converted into energy not served PDFs. The corresponding mean and percentile values show the 'likely' distributions in the next 24-hourly period. PDFs of daily totals are also computed. Besides, conditional PDFs of the load recovery initiation times given the load reduction at certain hour are also produced.

2) Generation Outputs: PDFs of generator hourly productions and costs, as well as total daily costs are computed.

3) Nodal Marginal Prices: PDFs of nodal marginal prices are produced for each hour in the considered 24-hourly period. Their expectations can be used as an indicator what the prices for rewarding generation and charging load customers will be next day.

4) Reliability Indices: Reliability indices relating to energy not served as well as frequency of customer interruptions and duration of interruptions are computed. For example, expected energy not supplied (*EENS*), expected frequency of interruptions (*EFI*) and expected duration of interruptions (*EDI*) are calculated as:

$$EENS = \sum_{y=1}^{Y}\sum_{t=1}^{T}\sum_{i=1}^{N}\sum_{s=1}^{s_4} Pc_i^s \big/ Y,$$
$$EFI = \sum_{y=1}^{Y}\sum_{t=1}^{T}\sum_{i=1}^{N}\sum_{s=1}^{s_4} \zeta_i^s \big/ Y$$
$$EDI = \sum_{y=1}^{Y}\sum_{t=1}^{T}\sum_{i=1}^{N}\sum_{s=1}^{s_4} \zeta_i^s \cdot D_i^s \big/ Y. \quad (25)$$

5) Financial Indicators: PDFs of load customer payments (*LC*), voluntary (*VLR*) and involuntary load reduction rewards (*IVLR*) are computed by hours and for the considered day. The latter curves are then used to quantify the financial risk of implementing the proposed demand response scheduling. The concept of value-at-risk (VaR) [30] was applied to measure the potentially 'low' revenues or 'excessive' payments.

Assuming network reward (*NR*) denotes any category of revenues, the corresponding cumulative distribution function (CDF_{NR}) is used to calculate the network reward NR_X that exceeds the network reward at the confidence level α, NR_a, with probability $1 - \alpha$. The value at risk is [31]:

$$VaR_a^{NR}(NR_X) = \inf\{NR_\alpha \in \mathrm{R} : CDF_{NRx}(NR_\alpha) \geq \alpha\} \quad (26)$$

Similarly, the *CDF* of any network cost (*NC*) can be used to determine value-at-risk at confidence level α. In this case, network cost NC_X that does not exceed the network cost at probability $1 - \alpha$, NC_{1-a}, is calculated as:

$$VaR_{1-a}^{NC}(NC_X) = \sup\{NC_{1-a} \in R : CDF_{NCx}(NC_{1-a}) \leq 1 - \alpha\}. \quad (27)$$

IV. Bulk Electric Power System

This section describes some practical aspects of the ampacity calculation of OHLs, modelling of wind farms, as well as the designed case studies.

TABLE I
Conductor Properties Modeled in IEEE-RTS Network

Name	*Rac (Ω/Km)*	*Configuration*	S_{NORM} *(MVA)*	$S_{EM\text{-}LONG}$ *(MVA)*
Dove (138kV)	0.1003 @ 25°C 0.1270 @ 75°C	Single bundle	95 [60°C]	138 [75°C]
Hawk (230kV)	0.1154 @ 25°C 0.1225 @ 75°C	Twin bundle	308 [60°C]	365 [75°C]

A. Thermal Ratings of Overhead Lines

The IEEE-RTS 96 test system does not provide any OHL data required for the RTTR calculations. A simple ACSR technology was assumed with conductor sizes that provide similar ratings to those in the IEEE-RTS 96 system with AAAC and ACSR conductors. Table I provides the information on the conductors used in the analysis. Under normal operation conductor temperature, T_c, is set to 60°C. A line is considered in emergency state when another transmission line connected at the same bus fails. The maximum conductor temperature in emergencies is set to 75°C based on avoidance of the conductor annealing [32].

B. Integration of Wind Farms

The power output of a wind turbine generator (WTG) is driven by the wind speed and the corresponding relationship is nonlinear. It can be described using the operational parameters of the WTG, such as cut-in, rated and cut out wind speeds. The hourly power output is obtained from the simulated hourly wind speed using the relations [33]:

$$P(V_m) = \begin{cases} 0, & 0 \leq V_m < V_{ci} \\ \left(A + B \times V_m + C \times V_m^2\right) \times P_r, & V_{ci} \leq V_m < V_r \\ P_r, & V_r \leq V_{mt} < V_{co} \\ 0, & V_m \geq V_{co} \end{cases} \quad (28)$$

where P_r, V_{ci}, V_r, and V_{co} are, respectively, rated power output, cut-in wind speed, rated wind speed and cut-out wind speed of the WTG, whilst V_m is simulated wind speed at hour t. The power output constants A, B and C are determined by V_{ci}, V_r, and V_{co}, as shown in [33]. All WTG units used in this study are assumed to have cut-in, rated, and cut-out speeds of 14.4, 36, and 80km/h, respectively. The failure rates and average repair times are assumed to be two failures/year and 44 hours.

C. Case Study Description

OHL thermal ratings are modelled as STR or RTTR, as shown in Table II below. Three seasons (winter, summer and fall),denoted as $\lambda_s = 1, 2, 3,$ are studied. The first day of the 50th peak week of the year is used for winter (hours: 8425-8449); the 2nd day of the 22nd week of the year is used for summer (hours: 3721-3744) and the 2nd day of the 32nd week is used for fall (hours: 5401-5424). Availability factor f_{RED}^s is a random number, whilst availability factor for load recovery f_{REC}^s varies in the specified range. Load

TABLE II
MODELING SCENARIOS OF DR METHODOLOGY

	S1	S2	S3	S4	S5	S6	S7	S8
p	STR	STR	STR	STR	RTTR	RTTR	STR	STR
λ_s	1,2,3	1	1,2,3	1	1	1	1	1
f^s_{RED}	0	1	1	1	0	1	0	1
f^s_{REC}	0	1	1	0-1.2	0	1	0	1
ϑ_{REC}	-	0	1	1	-	1	-	1
wg	0	0	0	0	0	0	1	1

recovery is based on either hourly emergency energy prices (i.e., $\vartheta_{REC} = 1$) or load profiles (i.e., $\vartheta_{REC} = 0$). The presence of wind generators is denoted by $wg=1$.

Eight scenarios are described in Table II. Scenario S1 is the base case, where the system is evaluated without DR scheduling and with standard thermal ratings for OHLs. Scenario S2 models load recovery by using the hourly load curve at each load point ($\vartheta_{REC} = 0$). Scenario S3 models all seasons and load recovery on the basis of expected marginal prices at each load point ($\vartheta_{REC} = 1$). Scenario S4 models time-varying load recovery profiles. Sensitivity studies are done here in order to assess the impact of different recovery sizes and profiles on DR performance. Factor f^s_{REC} is set from 0 to 1.2pu increasing in 0.2pu increments; the 1.2pu is taken as a high-risk scenario. Scenario S5 incorporates the RTTR of OHLs without DR operation, while Scenario S6 includes the DR scheduling. Finally, Scenario S7 incorporates wind farms without DR, while in Scenario S8 the benefits of demand response are evaluated incorporating wind generation ($wg=1$).

The original IEEE-RTS 96 was modified: all scenarios assume an increase in load by 1.2pu compared to the original load, as well as increase of 0.55pu and 0.6pu transmission capacity for the 138kV and 230kV levels, respectively, and 1.2pu in generation capacity. Next, the WTGs are connected at seven sites and it was assumed that they operate at power factor mode with power factor equal 35% [34]. Wind farms are designed to deliver 20% of the peak load [35], equivalent to 684MW on the studied power network. Geographically, 70% of the wind farms' maximum capacity is installed in the northern part of the network at buses 15, 17, 19, 20, 22, while in the southern part of the network, the remaining 30% of the wind capacity is installed to at buses 1, 2, 7, 8. The total wind farm capacity is 2394 MW obtained from a total number of 240 WTG, each representing a nominal capacity of 10MW. There is significant transmission utilization in this modified system as the bulk of the generating capacity is located mainly in the northern areas and considerable power is transferred from the north to the south aiming to represent the existing topology of the U.K. network. The analysis will study potential low wind output conditions in combination with unexpected network components failures.

V. CASE STUDY ANALYSIS

The IEEE-RTS 96 is composed of 38 lines circuits, 32 generating units and 17 load delivery points [36].

It is studied by using the algorithms developed in Matlab that make use of a modified version of Matpower and MIPS solver for the power flow calculations [37]. Essential study results on the eight scenarios related to the availability for load reduction, impact of nodal marginal prices, load recovery profile – availability, and impact of RTTR, DR and wind generation, are presented below.

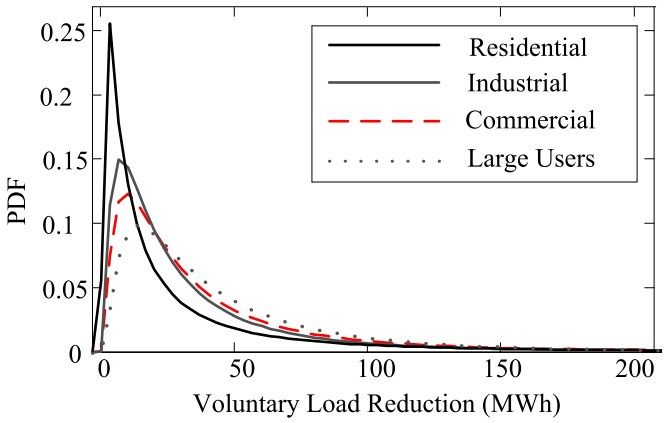

Fig. 3. Probability to respond to a DR signal for different customer types based on the voluntary load reduction amount at 17h00.

A. Customer Availability for Load Reductions

In this section, the impact of the availability of customers responding to a DR call is examined. Uncertainty in load availability for each customer type is given by equation (18). In particular, domestic customers' load reduction takes values from the entire possible range, while for industrial and commercial loads it is within the assumed window, *win=0.8-1pu*. Scenario 3 (S3) is used to evaluate the impact of customers responding to a DR on the *EENS*, mean and *VaR* values of voluntary (VLR) and involuntary load reductions (IVLR) – eqs. (12) and (13). For VLRs, Fig. 3 (generated over the entire MCS period) shows that the probability for residential loads to give 'small' response (up to 25 MWh) is much higher than to produce 'large' response (up to 50MWh).

However, industrial, commercial and large users are more likely to give 'larger' responses as they have bigger contracted amounts compared to residential users, and the uncertainty in response (if any) is much lower. For low load reductions, industrial loads have higher probability to respond than commercial and large users, while large users have the highest probability for larger amounts of load reductions; they are followed by commercial and industrial users.

The PDFs for voluntary (VL) and involuntary (IVL) load reductions for different hours in a day are illustrated in Fig. 4 and compared with the PDF of IVL without DR ($IVL^{NO\ DR}$). The results show that the probability of having IVL is reduced when doing DR (IVL^{DR}) with higher amounts (right side of x-axis), while the probability is much higher for low amounts of IVL. This clearly shows the effectiveness of voluntary DR on the EENS. In particular, the mean value of IVL^{DR} at 17h00 is around 60% less than the mean value of $IVL^{NO\ DR}$. A similar conclusion applies to all hours; for example, the mean of IVL^{DR} at 21h00 and 22h00 is, respectively, 61% and 60% lower when applying the voluntary DR. Applying

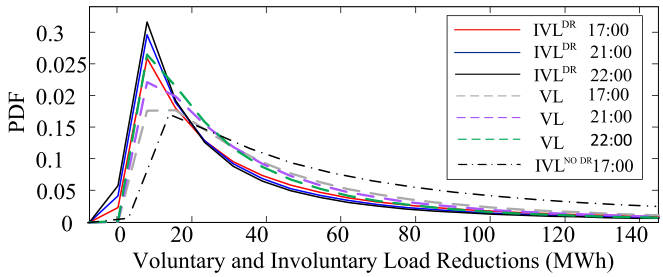

Fig. 4. Probability of voluntary and involuntary load reductions under DR for different hours in a day.

TABLE III
VAR VALUES OF CUSTOMERS COSTS AND REWARDS (K£)

Critical buses	*B6*		*B8*		*B14*	
	S1	S3	S1	S3	S1	S3
$VaR^{LC}_{50\%}$	31.43	19.59	55.13	22.91	57.55	41.72
$VaR^{LC}_{90\%}$	55.64	52.81	75.11	61.24	95.39	89.08
$VaR^{VLR}_{50\%}$	-	1.3	-	1.8	-	1.5
$VaR^{VLR}_{90\%}$	-	5.6	-	2.5	-	2.8
$VaR^{IVLR}_{50\%}$	600	240	578	320	480	252
$VaR^{IVLR}_{90\%}$	1344	420	1260	604	1284	546

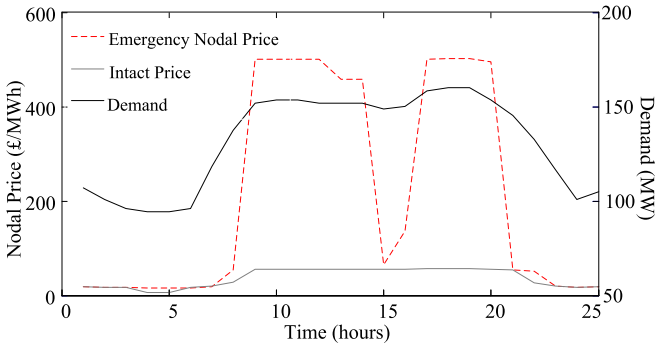

Fig. 5. Hourly marginal prices and demand curve under emergency for Bus 6.

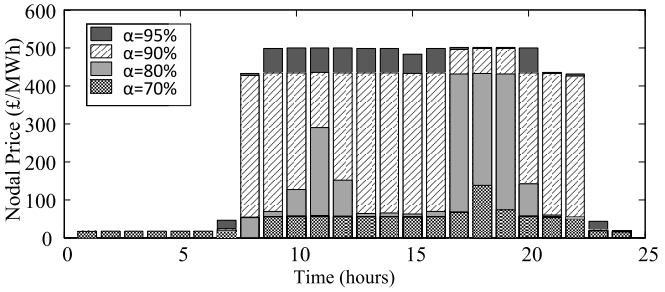

Fig. 6. Emergency marginal price for different confidence levels.

voluntary load reduction (VL) helps eliminate the need for involuntary one ($IVL^{NO\ DR}$), particularly when larger VL amounts are used. This is further highlighted when converting VL and IVL into the EENS index (see Table IV in Section V-B).

Table III shows the mean ($VaR_{50\%}$) and the 90% confidence VaR ($VaR_{90\%}$) for the costs for demand (LC), for VLR and IVLR revenues for the most critical load points (B6, B8 and B14) under scenarios S1 and S3. Both the $VaR^{LC}_{50\%}$ and $VaR^{LC}_{90\%}$ are much lower under S3 for all load points, since under DR, demand is recovered under cheaper nodal marginal prices.

In addition, $VaR^{VLR}_{90\%}$ is much larger than $VaR^{VLR}_{50\%}$ since marginal nodal prices are significantly higher under emergency conditions. Furthermore, the $VaR^{IVLR}_{50\%}$ is much lower under S3 than under S1, where it decreases by 60% for B6, 44% for B8 and 47% for B14. This also shows that voluntary DR significantly decreases the need for IVL (an average VOLL value was assumed for all customer types).

B. Impact of Nodal Prices on Reliability Analysis

Most DR studies would recover reduced load during load troughs and/or system normal if only network adequacy were looked at.

However, we have used the approach to investigate impact of hourly nodal prices on load recovery and customers' well-being. Fig. 5 shows an example of the nodal marginal price and the demand variation in time for the most frequently interrupted bus in the network (B6) under both intact and emergency conditions.

When no failures occur, load can be recovered almost at any time since intact prices do not change significantly with respect to load. However, nodal prices under emergency conditions may vary considerably. For instance, a significant shape difference between intact and emergency nodal prices is shown at 15h00. Our analysis has proven that the magnitude of the emergency nodal price can be almost 5 times higher than the intact one. Thus, scheduling of 'optimal' load recoveries based on marginal nodal prices has proven effective in providing system security and customer benefits. Furthermore, comparative studies were conducted to quantify the improvements from implementing load recovery under nodal marginal prices rather than under load profile only.

The hourly nodal price at bus B6 for different confidence levels is given in Fig. 6. In the event of an emergency at B6, TSOs may be provided with the illustrated confidence level dependent prices to decide which load recovery hour would be the most appropriate to restore load. For example, the TSO can know that if a violation occurs at 11h00, the load can be recovered between 13h00 and 16h00, since there is an 80% probability that the price will be between zero and 90£/MWh and a 90% probability that the price will be between zero and 420£/MWh. In this paper, a conservative confidence level of $\alpha = 95\%$ was selected. This gives flexibility to TSOs to apply operational decisions so they can guarantee making a profit for the demand customers for almost all nodal prices in the feasible range, since the load recovery will be at either the emergency nodal prices or (lower) intact prices.

The results presented in Table IV show that DR strategy under scenario S3 improves the reliability of the network in terms of EENS by 66% in winter ($\lambda_s = 1$) compared with S1, allowing for almost a 5% decrease in EENS compared to S2. The S3 strategy also substantially improves reliability indices

TABLE IV
RELIABILITY INDICES FOR SCENARIOS 1, 2 AND 3

S	EENS(MWh/day)			EDI(*10^{-2}h/day)			EFI(int/day)		
λ_s	1	2	3	1	2	3	1	2	3
S1	577	160.5	36.4	23.9	9.7	0.99	0.039	0.0156	0.00234
S2	206	59.2	12.9	23.2	9.2	0.57	0.0385	0.0154	0.00231
S3	196	42.8	4.8	23.3	8.5	0.35	0.0383	0.01532	0.00229

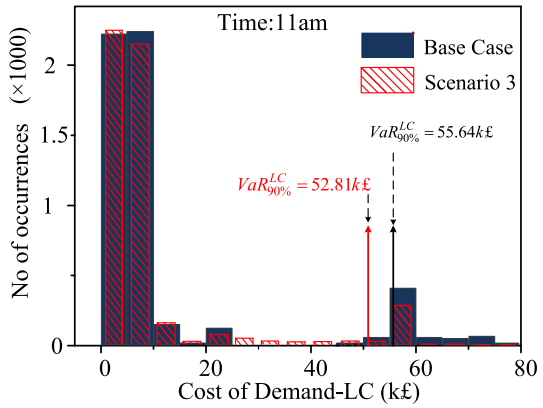

Fig. 7. Distribution of demand costs for load at Bus 6.

TABLE V
RELIABILITY INDICES FOR SCENARIO 4

f_{REC} (pu)	1.2	1	0.8	0.6	0.4	0.2
EENS(MWh/day)	205.8	196	192.34	191.13	191.08	188.12
EDI(h/day)	0.2334	0.2331	0.2330	0.229	0.227	0.227
EFI(int/day)	0.0386	0.0383	0.0383	0.038	0.038	0.0378

for summer ($\lambda_s = 2$) and fall ($\lambda_s = 3$), which demonstrates the effectiveness of the algorithm throughout the year.

In order to show the necessity to quantify the economic risk of DR operation, results for the base case S1 are compared to scenario S3 to investigate the VaR of the load cost (LC). Fig. 7 illustrates frequency of occurrence of various load costs seen at the most critical bus, B6, with and without DR. In particular, it is shown that there is a high variation in nodal costs at 11h00, resulting from outages of lines 12 and 13 that connect B6 with cheaper generators. Consequently, $VaR^{LC}_{90\%}$ is 55.64k£ under the base case, whereas it is only 52.81k£ under S3, which shows that DR can help reduce nodal costs by 5% (2.83k£). Clearly, both reliability and financial indices can be improved using nodal energy prices (S3) rather than the load profile only (S2).

C. Impact of Customer Availability to Recover the Load

The load recovery of a DR customer can be of different size compared to the corresponding load reduction. As a result, this can affect both the network performance and customer profits, as exemplified by scenario S4.

Assuming load recovery size is specified by availability factor f^s_{REC}, Table V shows an increase of around 5% in EENS for f^s_{REC} =1.2pu compared to f^s_{REC} =1pu. When load recovery sizes are lower than 100%, network reliability is improved compared to f_{REC}=1pu. This is due to the higher probability of implementing voluntary DR since less load recoveries are required. There is also a substantial decrease in reliability indices EDI and EFI.

TABLE VI
DIFFERENCE IN MEAN AND VAR FOR LC (£) AND PROFITS (£/KWH) S4 VS. S3

S5	S4-S3 Values			
	$VaR^{LC}_{50\%}$	$VaR^{LC}_{90\%}$	$VaR^{\pi}_{50\%}$	$VaR^{\pi}_{90\%}$
f_{REC}=1.2	+912	+1932	+0.05	+0.2
f_{REC}=0.8	-89	+775	+5.3	+8.1
f_{REC}=0.6	-101	-198	+6.3	+9.5
f_{REC}=0.4	-257	-2102	+8.8	+9.5
f_{REC}=0.2	-463	-2124	+10.2	+12.8

TABLE VII
IEEE RTS NETWORK EVALUATION WITH RTTR & DR

Scenarios		S3	S5	S6
Reliability indices	EENS(MWh/day)	196	475	183
	EFI (int/day)	0.0383	0.0381	0.0379
	EDI*10^{-2}(h/day)	23.31	23.34	23.18
Financial indices (k£)	$VaR^{LC}_{50\%}$	135.9	134.9	131.3
	$VaR^{LC}_{90\%}$	142.7	136.1	134.8
	$VaR^{VLR}_{50\%}$	1.6	-	1.2
	$VaR^{IVLR}_{50\%}$	2352	-	2196

Differences in the mean ($VaR_{50\%}$) and $VaR_{90\%}$ values for demand costs (LC) and customer profits (π) between scenarios S4 and S3 are shown in Table VI for different load recovery sizes f^s_{REC}. This table gives the cost and revenue differences following various load payback sizes compared to applying DR with a load payback of 100% for a winter day-ahead operation. For instance, when S4 is modeled with f_{REC} =1.2pu, the $VaR^{LC}_{50\%}$ is 912£ higher than under scenario S3. This is because as load recovery gets larger, the operating conditions become more difficult and the marginal prices increase, implying higher costs for demand. For low load recovery sizes, however, very high profits can be incurred (over 2,100£) as the demand cost VaR shows the largest decrease, thus suggesting a much lower probability of high LC.

D. Impact of RTTR and DR on Network Reliability and Customer Costs & Revenues

In scenario S5 only RTTR is used, whilst scenario S6 makes use of DR in conjunction with RTTR. Table VII shows that the more reliable and cheapest scenario is S6.

The use of RTTR and DR under S6 results in, respectively, 61% and 6.6% reduction in EENS compared with DR alone (S3) and with S5. Indices EFI and EDI are also improved. When RTTR is considered alone (S5), the greater utilization of the three most critical lines improves network performance by 18% compared to S1. Besides, the load cost index for S3 $VaR^{LC}_{50\%}$ is slightly higher than $VaR^{LC}_{50\%}$ for S5. This is because RTTR allows greater generation from cheaper units.

In terms of VLR and IVLR, both average values are lower under S6.

TABLE VIII
IEEE RTS NETWORK EVALUATION OF WIND FARMS & DR

Scenarios		S3	S7	S8
Reliability indices	EENS(MWh/day)	196	496	189
	EFI (int/day)	0.0383	0.0388	0.0383
	EDI*10^{-2}(h/day)	23.31	23.8	23.19
Financial indices (k£)	$VaR^{LC}_{50\%}$	135.9	135.3	129.3
	$VaR^{LC}_{90\%}$	142.7	141.9	136.8
	$VaR^{VLR}_{50\%}$	1.6	-	1.05
	$VaR^{IVLR}_{50\%}$	2352	-	2268

We can note that DR provides the greatest benefits since all indices are drastically improved with DR, whilst benefits are only slightly higher under RTTR.

E. Impact of Wind Farms and DR on Network Reliability and Customer Costs & Revenues

In scenario S7, only wind farms are used, whilst scenario S8 uses DR in conjunction with wind farms. Table VIII shows that the more reliable and less expensive scenario is S8; the wind farms contribute to improving network reliability by 4% in EENS compared with S3 alone. Besides, a considerable reduction in EDI is achieved, whilst frequency of interruptions, EFI, remains the same as under S3. If compared with S1, wind farms alone (S7) improve network performance by 14% due to wind farms' network reinforcements. Also, $VaR^{LC}_{50\%}$ for S3 is slightly higher than $VaR^{LC}_{50\%}$ for S7 as wind farms are considered to have near-zero marginal costs. When wind farms are used in conjunction with DR (S8), this has the best effect on network performance and customer costs & revenues. This is because DR implementation helps when wind output is low and network components fail. Next, when wind output is high, spillage can occur as there is not enough capacity on the network to transfer the total amount of wind, thus leading to congestion when using STR for OHL operation. This can result in a small reduction of EENS.

VI. CONCLUSION

A probabilistic methodology for optimal scheduling of load reductions/recoveries in a day-ahead planning of transmission networks is proposed in the paper. The methodology recognizes several types of uncertainties, and finds optimal demand response scheduling using the network security and customer economics criteria. Impacts of wind generation and real-time thermal ratings of overhead lines are also studied.

The developed case studies have demonstrated that the value of optimal demand scheduling combined with real-time thermal ratings can be significant when using nodal marginal prices compared to using the hourly loads only. In particular, both reliability and financial metrics can be improved by a factor of around 66% for expected energy not served and around 5% for value at risk for costs of demand. Improvements in other reliability indicators and expected generation costs were also observed. Nonetheless, selection of the reliability indicator to base the operational decisions on demand scheduling can be of highest importance; having multiple indices can therefore help system operators to make more informed decisions on 'best' demand response practice. As a final comment, the consistent use of a probabilistic approach to model various network uncertainties and variability of nodal marginal prices provides a superior analysis compared to traditional analytical techniques.

The future work considers inclusion of optimal energy storage scheduling to increase system reliability. Combined impact of energy storage, demand response and wind generation will be studied in greater detail.

REFERENCES

[1] P. Denholm and M. Hand, "Grid flexibility and storage required to achieve very high penetration of variable renewable electricity," *Energy Pol.*, vol. 39, no. 3, pp. 1817–1830, 2011.

[2] D. T. Nguyen, M. Negnevitsky, and M. de Groot, "Pool-based demand response exchange—Concept and modeling," *IEEE Trans. Power Syst.*, vol. 26, no. 3, pp. 1677–1685, Aug. 2011.

[3] A. S. Deese, E. Stein, B. Carrigan, and E. Klein, "Automation of residential load in power distribution systems with focus on demand response," *IET Gener. Transm. Distrib.*, vol. 7, no. 4, pp. 357–365, Apr. 2013.

[4] P. Wang, Y. Ding, and Y. Xiao, "Technique to evaluate nodal reliability indices and nodal prices of restructured power systems," *IEE Proc. Gener. Transm. Distrib.*, vol. 152, no. 3, pp. 390–396, May 2005.

[5] M. Fotuhi-Firuzabad and R. Billinton, "Impact of load management on composite system reliability evaluation short-term operating benefits," *IEEE Trans. Power Syst.*, vol. 15, no. 2, pp. 858–864, May 2000.

[6] E. Karangelos and F. Bouffard, "Towards full integration of demand-side resources in joint forward energy/reserve electricity markets," *IEEE Trans. Power Syst.*, vol. 27, no. 1, pp. 280–289, Feb. 2012.

[7] D. T. Nguyen, M. Negnevitsky, and M. de Groot, "Modeling load recovery impact for demand response applications," *IEEE Trans. Power Syst.*, vol. 28, no. 2, pp. 1216–1225, May 2013.

[8] N. Ruiz, I. Cobelo, and J. Oyarzabal, "A direct load control model for virtual power plant management," *IEEE Trans. Power Syst.*, vol. 24, no. 2, pp. 959–966, May 2009.

[9] A. Molina-Garcia, F. Bouffard, and D. S. Kirschen, "Decentralized demand-side contribution to primary frequency control," *IEEE Trans. Power Syst.*, vol. 26, no. 1, pp. 411–419, Feb. 2011.

[10] C. L. Su and D. Kirschen, "Quantifying the effect of demand response on electricity markets," *IEEE Trans. Power Syst.*, vol. 24, no. 3, pp. 1199–1207, Aug. 2009.

[11] R. Billinton and W. Li, *Reliability Assessment of Electrical Power Systems Using Monte Carlo Methods*. London, U.K.: Plenum, 1994.

[12] J. Schachter and P. Mancarella, "A short-term load forecasting model for demand response applications," in *Proc. IEEE 11th Int. Conf. Eur. Energy Market (EEM)*, Krakow, Poland, 2014, pp. 1–5.

[13] LE 2013, "The value of lost load (VoLL) for electricity in Great Britain: Final report for OFGEM and DECC London economics," Jul. 2013.

[14] ER. P27, "Current rating guide for high voltage overhead lines operating in the UK distribution system," Energy Network Association, London, U.K., 1986.

[15] *IEEE Standard for Calculating the Current-Temperature of Bare Overhead Conductors*, IEEE Standard 738-2006, 2007, pp. 1–59.

[16] British Atmospheric Data Centre. *User Guide for Extracting MIDAS Data and Metadata*. Accessed on Nov. 12, 2013. [Online]. Available: http://badc.nerc.ac.uk/data/ukmo-midas/WPS.html

[17] J. M. Arroyo and F. D. Galiana, "Energy and reserve pricing in security and network-constrained electricity markets," *IEEE Trans. Power Syst.*, vol. 20, no. 2, pp. 634–643, May 2005.

[18] M. S. Bazaraa, J. J. Jarvis, and H. D. Sherali, *Linear Programming and Network Flows*, 4th ed. Hoboken, NJ, USA: Wiley, 2010.

[19] I. J. Perez-Arriaga and C. Meseguer, "Wholesale marginal prices in competitive generation markets," *IEEE Trans. Power Syst.*, vol. 12, no. 2, pp. 710–717, May 1997.

[20] K. Singh, N. P. Padhy, and J. Sharma, "Influence of price responsive demand shifting bidding on congestion and LMP in pool-based day-ahead electricity markets," *IEEE Trans. Power Syst.*, vol. 26, no. 2, pp. 886–896, May 2011.

[21] X. Cheng and T. J. Overbye, "An energy reference bus independent LMP decomposition algorithm," *IEEE Trans. Power Syst.*, vol. 21, no. 3, pp. 1041–1049, Aug. 2006.
[22] S. Wong and J. D. Fuller, "Pricing energy and reserves using stochastic optimization in an alternative electricity market," *IEEE Trans. Power Syst.*, vol. 22, no. 2, pp. 631–638, May 2007.
[23] D. S. Kirschen, K. R. W. Bell, D. P. Nedic, D. Jayaweera, and R. N. Allan, "Computing the value of security," *IEE Proc. Gener. Transm. Distrib.*, vol. 150, no. 6, pp. 673–678, Nov. 2003.
[24] G. Dorini, P. Pinson, and H. Madsen, "Chance-constrained optimization of demand response to price signals," *IEEE Trans. Smart Grid*, vol. 4, no. 4, pp. 2072–2080, Dec. 2013.
[25] C. Chen, J. Wang, and S. Kishore, "A distributed direct load control approach for large-scale residential demand response," *IEEE Trans. Power Syst.*, vol. 29, no. 5, pp. 2219–2228, Sep. 2014.
[26] A. Abdollahi, M. P. Moghaddam, M. Rashidinejad, and M. K. Sheikh-El-Eslami, "Investigation of economic and environmental-driven demand response measures incorporating UC," *IEEE Trans. Smart Grid*, vol. 3, no. 1, pp. 12–25, Mar. 2012.
[27] M. H. Albadi and E. F. El-Saadany, "A summary of demand response in electricity markets," *Elect. Power Syst. Res.*, vol. 78, no. 11, pp. 1989–1996, 2008.
[28] E. Agneholm and J. Daalder, "Load recovery in different industries following an outage," *IEE Proc. Gener. Transm. Distrib.*, vol. 149, no. 1, pp. 76–82, Jan. 2002.
[29] G. Strbac, E. D. Farmer, and B. J. Cory, "Framework for the incorporation of demand-side in a competitive electricity market," *IEE Proc. Gener. Transm. Distrib.*, vol. 143, no. 3, pp. 232–237, May 1996.
[30] National Grid. (Jul. 2013). *National Grid EMR Analytical Report*. [Online]. Available: https://www.gov.uk/government/uploads/system/uploads/attachment_data/file/223655/emr_consultation_annex_e.pdf
[31] A. Shapiro and S. Basak, "Value-at-risk based risk management: Optimal policies and asset prices," *Rev. Financ. Stud.*, vol. 14, no. 2, pp. 371–405, 2001.
[32] K. Kopsidas, S. M. Rowland, and B. Boumecid, "A holistic method for conductor ampacity and sag computation on an OHL structure," *IEEE Trans. Power Del.*, vol. 27, no. 3, pp. 1047–1054, Jul. 2012.
[33] P. Giorsetto and K. F. Utsurogi, "Development of a new procedure for reliability modeling of wind turbine generators," *IEEE Trans. Power App. Syst.*, vol. PAS-102, no. 1, pp. 134–143, Jan. 1983.
[34] Dept. Energy Climate Change, "Digest of UK energy statistics: Renewable sources of energy," 2014, pp. 157–193.
[35] K. Soren, M. Poul-Eric, and A. Shimon, *Wind Energy Implications of Large-Scale Deployment on the GB Electricity System*, Roy. Acad. Eng., London, U.K., 2014, p. 72.
[36] C. Fong, S. Haddad, and D. Patton, "The IEEE reliability test system-1996," *IEEE Trans. Power Syst.*, vol. 14, no. 3, pp. 1010–1020, Aug. 1999.
[37] R. D. Zimmerman, E. M.-S. Carlos, and D. Gan, "MATPOWER: A MATLAB power system simulation package, version 3.1b2, user's manual," Power Syst. Eng. Res. Center (PSERC), New York, NY, USA, Tech. Rep. 2006, 2011.

Konstantinos Kopsidas (M'06) received the B.Eng. degree in electrical engineering from the Institute of Piraeus, Athens, Greece, in 2002; the B.Eng. degree (First Class) in electrical and electronic engineering from the University of Manchester Institute of Science and Technology, U.K., in 2004; and the M.Sc. (with distinction) and Ph.D. degrees in electrical power engineering from the University of Manchester in 2005 and 2009, respectively. Since 2011, he has been a Lecturer with the School of Electrical and Electronic Engineering, University of Manchester, with main research interests on plant modeling and reliability and adequacy.

Alexandra Kapetanaki (S'12) received the M.Eng. degree in electrical engineering and computer science from the National Technical University of Athens, Greece, in 2011. She is currently pursuing the Ph.D. degree with the Electrical Energy and Power Systems Group.

Her current research interests include optimization of power system operation, stochastic modelling, risk management, and electricity markets.

Victor Levi (S'89–M'91–SM'13) received the M.Sc. and Ph.D. degrees in electrical engineering from the University of Belgrade, Belgrade, Yugoslavia, in 1986 and 1991, respectively.

From 1982 to 2001, he was with the University of Novi Sad, Novi Sad, Yugoslavia, where he became a Full Professor in 2001. He was with the University of Manchester, Manchester, U.K., from 2001 to 2003, and then with United Utilities and Electricity North West from 2003 to 2013. In 2013, he rejoined the University of Manchester.